View metadata, citation and similar papers at core.ac.uk
brought to you by CORE
provided by NASA Technical Reports Server

NASA Technical Memorandum 100868

Thermal Distortion Analysis of the Space Station Solar Dynamic Concentrator

Jeffrey J. Trudell
National Aeronautics and Space Administration
Lewis Research Center
Cleveland, Ohio

Vithal Dalsania
W.L. Tanksley & Associates
Lewis Research Center
Cleveland, Ohio

Joseph F. Baumeister
Analex Corporation
Lewis Research Center
Cleveland, Ohio

and

Kent S. Jefferies
National Aeronautics and Space Administration
Lewis Research Center
Cleveland, Ohio

Prepared for the
23rd Intersociety Energy Conversion Engineering Conference
cosponsored by the ASME, AIAA, ANS, SAE, IEEE, ASC, and AIChE
Denver, Colorado, July 31—August 5, 1988

NASA

(NASA-TM-100868) THERMAL DISTORTION ANALYSIS OF THE SPACE STATION SOLAR DYNAMIC CONCENTRATOR (NASA) 25 p CSCL 10B
N88-25475
Unclas
G3/20 0149244

Trade names or manufacturers' names are used in this report for identification only. This usage does not constitute an official endorsement, either expressed or implied, by the National Aeronautics and Space Administration.

THERMAL DISTORTION ANALYSIS OF THE SPACE STATION SOLAR DYNAMIC CONCENTRATOR

Jeffery J. Trudell
National Aeronautics and Space Administration
Lewis Research Center
Cleveland, Ohio 44135

Vithal Dalsania
W.L. Tanksley & Associates
Lewis Research Center
Cleveland, Ohio 44135

Joseph F. Baumeister
Analex Corporation
Lewis Research Center
Cleveland, Ohio 44135

and

Kent S. Jefferies
National Aeronautics and Space Administration
Lewis Research Center
Cleveland, Ohio 44135

E-4090

SUMMARY

A method has been developed to evaluate the thermal distortion of the Space Station Solar Dynamic Concentrator and the effects of thermal distortion on concentrator optical performance. The analytical method includes generating temperature distributions with TRASYS and SINDA models, interfacing the SINDA results with the SINDA-NASTRAN Interface Program (SNIP), calculating thermal distortion with a NASTRAN/PATRAN finite element model, and providing flux distribution maps within the receiver with the ray-tracing OFFSET program. Temperature distributions, thermally induced slope errors, and flux distribution maps within the receiver are discussed. Results during a typical orbit indicate that temperatures of the hexagonal panels and triangular facets range between -18 °C and 99 °C (-1 to 210 °F), facet rotations are less than 0.2 mrad, and a change in facet radius due to thermal flattening is less than 5 percent. The predicted power loss with thermal distortion effects was less than 0.3 percent. The thermal distortion of the Solar Dynamic concentrator has negligible effect on the flux distribution within the receiver cavity.

INTRODUCTION

To generate power for the Space Station, NASA will use both Photovoltaic (PV) and Solar Dynamic (SD) power generation systems. Four PV modules will provide 75 kWe for the Phase 1 Space Station. Two SD modules are being developed to provide an additional 50 kWe for the Phase 2, 125 kWe Station. The SD power generation system is more than 4 times more efficient in converting thermal energy to electrical power than the PV system. Consequently, the SD system provides a 60 percent reduction in drag per unit power thus reducing the amount of reboost propellant required to maintain the Space Station orbit. The closed

Brayton cycle (CBC) SD system collects solar energy to heat a working fluid, which in turn drives a turbine to rotate an electric generator. A thermal energy storage medium is required to heat the working fluid during the 28 to 36 min eclipse portion of the orbit.

To collect and focus sunlight for a 25 kWe SD module, NASA will develop a large solar concentrator that will provide a distributed solar flux within a heat receiver cavity. In order to achieve appropriate flux distribution within the heat receiver cavity, concentrator mirror surface accuracy and pointing accuracy tolerances are tightly controlled. Identified error sources that will influence the optical performance of the SD concentrator while on-orbit include facet alignment in a 1-g environment, facet manufacturing errors including slope error and specular reflectance, receiver to concentrator alignment, and thermal distortion. To maintain its optical performance over its 10 yr lifetime, the SD concentrator must be durable enough to withstand the harsh environment of the Space Station's low earth orbit (LEO). The LEO environment includes degradation of optical and structural surfaces from atomic oxygen, ultra-violet (UV) radiation, and micrometeoroid impacts, and a considerable number of thermal cycles due to solar illumination for approximately 60 min of a 95 min orbit.

This report discusses the method developed to determine the thermal distortion of the SD concentrator as well as the thermal distortion effects on concentrator optical performance. A brief description of the SD concentrator is first provided to help the reader understand the concentrator design. The method to determine the thermal distortion is then described, including descriptions of the thermal and structural models used in the analysis. Finally, the results of the thermal and structural analysis, and the effects of thermal distortion on optical performance are presented.

SD CONCENTRATOR DESCRIPTION

The SD concentrator is one of the eight major assemblies of the Space Station's SD Module as shown in figure 1. The SD concentrator is subdivided into 19 hexagonal panels sized to fit into the Space Shuttle's payload bay. The SD concentrator is an offset parabolic configuration in which the flat, hexagonal (hex) panels are fastened together by latches so that each panel lies on a paraboloid. The primary advantages of the offset parabolic and hex panel design concepts are the low mass moment of inertia of the SD module about the Space Station's transverse boom and the compactness of the stowed SD module which enables packaging of two complete modules in the Shuttle payload bay. An offset reflector does cause larger cosine losses than a symmetrical Newtonian concept and desirable symmetrical flux distributions are also more difficult to achieve (ref. 1). The concentrator reflective surface area is comprised of 456 facets, 24 facets per hex panel. The hex panels are supported by a nine strut support structure. Three of the struts provide stiffness to the hex panels and the other six struts attach the concentrator assembly to the receiver interface ring. The receiver is tilted approximately 51° to improve the circumferential flux distribution on the heat receiver cavity wall. The thermal design strategy of the SD concentrator includes using low absorptance and emmittance surface coatings or blankets to control component temperatures and selecting materials with a very low coefficient of thermal expansion to reduce thermal distortions.

The concentrator analyzed for this report was designed and developed by the Harris Corporation, Government Aerospace Systems Division (ref. 2). NASA initiated the Advanced Development (AD) effort with Harris to develop and demonstrate the most effective means of collecting and focusing solar energy to be used in a power generation system for the Space Station. The AD concentrator assembly is mapped to a spherical surface rather than the ideal parabolic surface. The spherically shaped AD concentrator geometry was selected for this study because of the availability of Harris' detailed drawings. The AD concentrator's spherical surface shown in figure 2 allows the hex panels to be mapped equally spaced on a sphere. Note that the projected view shown in figure 2 distorts the appearance of the equally spaced panels. The equal spacing of the hex panels reduced fabrication costs by decreasing the number of unique latch configurations and drawings. The panel designations, numbers from 1 to 19, referred to in the body of this report are also shown in figure 2.

The details of a flat, hexagonal panel are shown in figure 3. A hexagonal panel is comprised of twelve, rectangular cross section graphite fiber reinforced epoxy (GFRP) box beams. The 2-m length box beams are joined and bonded together at the hub and six corner points by shear plates and corner fitting assemblies. The GFRP box beams have a high stiffness to weight ratio, high strength to weight ratio, and a very low coefficient of thermal expansion (-0.9×10^{-6} cm/cm/C). The top and bottom GFRP shear plates provide the load path between the box beams at the six corners and the hub. The aluminum corner fittings define the hexagonal panel geometry and provide the attachment point for the aluminum latches (ref. 3).

To concentrate the sun's rays into the heat receiver, 24 mirrored triangular facets are mounted to each hexagonal panel with three standoff/flexure assemblies, one near each corner of the facet. The standoff/flexure assemblies shown in figure 4 isolate the facets from loads imposed by box beam distortions and allow for alignment of individual facets to reflect solar flux into the heat receiver cavity. The facets have varying spherical radii of curvature and are tilted within the panel frames depending upon their specific location on the concentrator. The triangular facets measure approximately 1 m on a side and have surface contour radii of 1921, 2181, 2441, or 2702 cm (756.25, 858.75, 961.25, or 1063.75 in.) for the AD concentrator as shown in figure 5. Four radii were chosen instead of 456 unique radii facets for the AD concentrator based on a slight increase in slope error, but a large decrease in facet manufacturing (tooling) costs. Each facet is made of two GFRP facesheets bonded to aluminum honeycomb core. The vapor deposited reflective and protective surfaces consist of aluminum with a magnesium fluoride or silicon oxide coating. Aluminum, although less reflective, was selected over silver for the AD concentrator because of its durability in the terrestrial environment. The specular surface for the reflective coating is provided by an epoxy rich layer of graphite vail on the facesheet and a polished surfaced caul plate (ref. 4).

ANALYSIS

The analytical method developed to evaluate the thermal distortion of the concentrator and the effects of thermal distortion on concentrator optical performance includes performing four major analysis tasks: (a) thermal analysis; (b) interfacing the thermal and structural models; (c) structural analysis; and (d) optical analysis. The analytical method was developed to provide an independent assessment of the Harris concentrator design. The analytical method

includes performing thermal analysis with the Thermal Radiation Analysis System (TRASYS) (ref. 5) and the System Improved Numerical Differencing Analyzer (SINDA) (ref. 6) to predict the temperatures of the concentrator's components. The thermal results are then interfaced to the structural model of the concentrator with the SINDA-NASTRAN Interface Program (SNIP) (ref. 7). The thermal distortion of the concentrator is calculated with a MSC/NASTRAN (NASA Structural Analysis Program) (ref. 8) finite element model. Energy distributions within the receiver cavity are determined with the ray-tracing OFFSET program (ref. 9). Finally, the thermal, structural, and optical results are processed with PATRAN (ref. 10) to provide contour plots of temperature distributions, displacements, facet rotations, and receiver flux distribution maps. Eight different programs were used to calculate the thermal distortion effects on optical performance of the SD concentrator as shown in figure 6. The eight programs include four commercially available programs--TRASYS, SINDA, MSC/NASTRAN, and PATRAN,-- and four FORTRAN programs developed at NASA Lewis -- SNPCRD, SNIP, CONRMS, and OFFSET. Also shown is the input and output of each of the programs. The following sections describe the four major analysis tasks and the programs used to perform the analysis in greater detail.

Thermal Analysis

The thermal analysis was performed by developing a geometric math model (GMM) for TRASYS and a thermal math model (TMM) for SINDA to predict the temperatures of the concentrator's components. TRASYS predicts the heating rates from environmental radiant heat sources and the interchange of radiation of the node network. SINDA is a generalized thermal analysis program that solves a lumped parameter representation of physical problems governed by diffusion-type equations as resistor-capacitor (R-C) network representations of thermal systems.

To predict the temperatures of the concentrator, both the GMM and TMM of the concentrator consisted of one detailed and 18 simplified hex panels. The detailed panel components included facets, box beams, corner fitting assemblies, shear plates, and latches, while the simplified panel was represented by six oversized facets. Using 18 simplified panels greatly reduced the spatial resolution and complexity of the concentrator model while still maintaining approximate reflected and radiative interactions of all 19 panels. Temperatures of the entire concentrator are obtained by making 19 TRASYS and SINDA runs with the detailed panel located in each of the 19 locations.

Figure 7 shows the concentrator GMM, as well as the detailed panel GMM, used to provide the heating rates and radiation conductors for the concentrator TMM. The total number of nodes for the concentrator GMM was 255, of which 146 are for the detailed panel, 108 for the simple panels and one node for space. The majority of the detailed panel GMM consisted of 24 facets (48 nodes) and 12 box beams (48 nodes). Four nodes were used to represent the four sides of the rectangular cross section box beam. The properties of the box beams and back surfaces of the facets were similar to those of KAPTON tape to represent the thermal control coating. The rest of the detailed panel GMM consisted of the top and bottom corner shear plates (36 nodes), center shear plates (6 nodes), and 2 latches (8 nodes). The simple panel GMM used six oversized facets to represent the equivalent area as an entire hex panel. The model was

assumed to be in a 250 nm altitude circular orbit when the sun is in the plane of the orbit ($\beta = 0°$), which has a period is 93.7 min with 35.7 and 58.0 min of eclipse and sunlight, respectively. A comparison of other orbit inclinations indicated that $\beta = 0°$ created the maximum concentrator component temperatures.

The TMM also consisted of one detailed and 18 simplified panels. The total number of nodes for the concentrator TMM was 165, of which 146 were for the detailed panel, 18 for the simple panels, and one node for space. The detailed panel consisted of 24 facets (24 nodes), 12 box beams (48 nodes), 12 corner and 2 center shear plates (14 nodes), 6 corner fitting assemblies (18 nodes), and 2 latches (2 nodes). Each of the 18 simple panels consisted of 6 oversized facets lumped together (18 nodes). To provide preliminary temperature distributions during an intermediate point of the study, the concentrator GMM and TMM included only beams and facets. Models of the shear plates and corner fitting assemblies were added later to model the conduction path at the panel corners. Modeling the conduction path at the panel corners reduced the box beam temperatures and temperature gradients.

Figure 8 shows the average facet and box beam temperatures as a function of time for panels 1, 8 and 14. At each time increment, the average facet and box beam temperatures were calculated by averaging the 24 facet and 48 box beam SINDA nodal temperatures on each panel. The box beam temperatures ranged between 12 and 79 °C (54 and 174 °F) after the temperatures reached cyclic steady-state by the third orbit. The maximum temperatures of the box beams, as well as the latch, corner fittings, and shear plates, all occurred approximately 57 min into the 58 min sunlit portion of the orbit. The maximum and minimum temperatures of the facets (99 to -18 °C or 210 to -1 °F), and simple panels (119 to -94 °C or 247 to -137 °F), occurred earlier at 42 and 30 min, respectively, into the sunlit portion of the orbit. The simple panels provided average approximations of typical facet temperatures, while providing close approximations of the reflected heating rates from all other sources. The worst box beam temperature gradient from one beam side to another was 1.51 °C/cm (6.9 °F/in.). The worst gradients occurred just before the eclipse portion of the orbit and approximately 12 min into the sunlit portion of the orbit.

Interfacing the Thermal and Structural Models

To predict the thermal distortions of the concentrator required mapping the temperature results from the thermal analysis to the finite element model. To allow the thermal and structural analysts to work independently and to eliminate the labor intensive task of relating specific thermal nodes to specific structural elements, the SINDA to NASTRAN Interface Program (SNIP) was used to correlate the SINDA and NASTRAN concentrator models. SNIP is a FORTRAN computer program that generates NASTRAN thermal load cards for NASTRAN plate, shell, bar, and beam elements with the temperature results from SINDA or any other thermal analyzer program and with geometric data (ref. 7). SNIP uses a geometric search routine and a numerical coding scheme to relate thermal model nodes to structural nodes. SNIP then calculates element temperatures based on a weighted average of temperatures of the thermal nodes related to each element. To reformat and add geometric data to the SINDA temperature results, the FORTRAN program SNPCRD was developed at NASA Lewis to create the input file of thermal node data cards for SNIP as shown in figure 6. In addition, SNPCRD created PATRAN files to plot the temperature distributions across the concentrator.

To interface the SINDA and NASTRAN models of the concentrator, SNIP required that the geometric data (X, Y, and Z coordinates) be assigned to each nodal temperature and that temperature gradients be determined for each node. The geometric data and temperature gradients are not provided by SINDA and were added by SNPCRD. The thermal load cases for the concentrator finite element generated by SNPCRD consisted of 798 node data cards: 24 facets, 12 box beams, and 6 corner fitting assemblies for each of the 19 panels. SNPCRD creates the input node data cards for SNIP by obtaining the node numbers and nodal temperatures of the facets, box beams, and corner fitting assemblies at a point in time during an orbit, assigning X, Y, and Z coordinates to the nodal temperatures by calculating each component's centroid, and determining the appropriate nodal temperature gradients. The centroids of each of the SINDA nodes (components) were calculated using the coordinates and dimensions from the Harris Corporation's concentrator drawings. To provide the box beam temperatures, SNPCRD averaged the four SINDA nodes representing the four box beam sides, and to provide box beam temperature gradients, SNPCRD subtracted the top and bottom and left and right box beam nodal temperatures. A local coordinate system for each box beam was developed in order to determine the proper sign and orientation of the temperature gradients in the structural elements.

The structural analysis required temperatures and temperature gradients of the concentrator's facets, box beams, and standoffs to determine the thermal distortions of the concentrator. Since the facets are attached to the hex panels with standoff/flexure assemblies, rotations of the hex panels and deflections of the the standoffs will misalign the facets. In addition, initial structural results indicated that the temperature gradients across and through the box beams cause the largest deflections and therefore temperature gradients through the box beams were calculated. By selecting the appropriate qualification and numerical coding parameters that relate the thermal and structural models, SNIP generated NASTRAN element thermal load cards for the facets, box beams, and standoffs. Note that SNIP produced a weighted average standoff temperature based on the temperatures of the nearest facet and hex panel corner fitting assembly. The temperatures of the facets and corner fitting assemblies were available from the thermal model, and having SNIP determine the standoff temperature avoided the effort of adding standoffs to the thermal model.

Structural Analysis

The structural analysis was performed using PATRAN and NASTRAN and thermal load cases produced by SNIP. NASTRAN is a general purpose computer program for structural analysis using the finite element method (ref. 8). NASTRAN is used to perform a steady state linear static analysis to determine the displacement vectors and rotations of the hex panels and facets. The primary results of interest are the displacements and rotations of the facets. No calculations are made to recover stresses in the elements associated with the thermal loads. PATRAN, a finite element pre- and post-processor engineering software package, was used to interactively create the concentrator finite element model and graphically evaluate the results. PATRAN was used to post-process the output data by creating contour plots of displacements, facet rotations, temperature distributions, and receiver flux distribution maps.

A concentrator finite element model predicts the rotations and deflections of the facet corners under thermal loads and a separate finite element model of a facet predicts the change of radius of curvature for each of the four facet

radii based upon thermal loads of a detailed facet thermal model. The initial structural analysis results indicated that the facets move independently of the hex panel, and therefore, the facets were modeled separately to reduce the number of nodes in the concentrator model. Deflections, rotations, and flattening of facets create thermally induced slope errors by changing the normal direction of points on a facet. The implicit combination of the rotations, deflections, and thermal flattening of the facets will be performed in the optical analysis.

The concentrator finite element model is constructed with 19 identical hex panels. The hex panel shown in figure 9 includes beams, facets, flexure assemblies, standoffs, latches, and support structure. Each box beam is modeled using four equal length bars or 204 bar elements per panel. Each facet is modeled using three triangular plate elements or 72 triangular plate elements per panel. To model the facets and box beams requires 223 nodes. The flexure assemblies are modeled with rigid links and bar elements with pseudo flexibilities to simulate the elasticity of the entire standoff/flexure assembly.

Bar elements were used instead of plate elements to represent the box beams of the hex panels in the finite element model because they limit the number of MSC/NASTRAN nodes without loss of accuracy, the modeling of the flexure/standoff assemblies is made simpler, and because SNIP can provide both temperatures and temperature gradients through the bar's cross section. In addition, the concentrator can be modeled using simplified facet-to-hex-panel junctions rather than modeling the actual flexure/standoff assembly as shown in figure 9. The standoffs are assumed to be attached to the facet corners with a single bar element of the equivalent stiffness of the standoff/flexure assembly and a rigid bar to significantly reduce the number of nodes required. In the actual design, a standoff is attached to the facet approximately 7.0 cm (2.75 in.) from the facet corner. To allow the standoffs to be connected at the facet corners in the finite element model, the actual facet corners are shifted toward the center of the facet to the approximate standoff-facet connection point. Consequently, the facet corners are located only approximately in the finite element model and will be modified with the actual locations for the optical analysis. All the other hex panel components are modeled in sufficient detail to accurately handle the thermal loads.

The nineteen panels now have to be interconnected to form a single structure. To duplicate the single hex panel at 19 locations, the X, Y, and Z coordinates of three points in space were obtained from the Harris drawings. Nineteen duplications of the panel were created and appropriately placed using a PATRAN command. The panels are connected using bar elements to represent latch joints. The latches are modeled using four bar elements connected together at one end to a node point to represent a ball joint as shown in figure 10. Note that rigid elements are used to connect the latch ends to the hex panel. This is necessary to accurately locate the connections of a structure modeled using bar elements (line type elements). The ball joint is modeled by releasing the rotating degrees of freedom on all four bar ends connected at the junction node. There are 140 nodes and 312 bar elements to represent the latches and support struts. The concentrator is attached to a tubular strut structure. The junction of strut structure to the concentrator and of the strut structure to the receiver is assumed to be pinned. The node points representing the receiver attachment are assumed restrained in all six directions.

Optical Analysis

An optical analysis was performed to determine the effects of thermal distortion on the concentrator optical performance. Two FORTRAN programs, CONRMS and OFFSET, written by the authors were used to evaluate the effects of thermal distortion on concentrator optical performance. CONRMS combines the absolute value of the rotations for each grid point on the facets to provide an approximate rotational value for the facets, hex panels, and concentrator. OFFSET is a detailed ray-tracing computer code that models the offset solar collector to predict receiver cavity solar flux distributions. Inputs to OFFSET include the displaced facet coordinates and the change in facet radius of curvature due to thermal flattening.

CONRMS is a FORTRAN program that converts the displacement data of the 456 facets into a rotational value for the facets, panels, and concentrator (an approximate mispointing error value). For each of the four node points that define a facet, CONRMS adds the squares of the rotations about the X and Y axes. The squared rotations of the four node points are then added together, with the square root of the sum representing the facet root-mean-square (RMS) value or mispointing error. Similarly, the squared rotations of the four node points of each of the 24 facets per panel are added together, with the square root of the sum defined to be the panel RMS value. The concentrator RMS value is simply the square root of the sum of the squared rotations of the four node points per facet for all 456 facets. The input file to CONRMS is generated by NASPAT (ref. 10), which reformats the NASTRAN displacement vectors and rotations into a PATRAN plot file. After computing the facet RMS values, the displacement output file from NASPAT is modified by replacing the last column with the RMS rotations of the facets. This modification provides a means to plot the RMS values with PATRAN. CONRMS also calculates the final coordinates of the facet corners for input into OFFSET. CONRMS calculates the coordinates of the three facet corners by adding the x, y, and z deflections from the NASPAT output file to the actual coordinates of each of the 456 facets as supplied on the Harris drawings.

OFFSET was developed at NASA Lewis to model the offset solar collector for the Space Station Solar Dynamic electric power system. This model traces rays from 50 points on the face of the Sun to ten points on each of 456 collector facets. Ray reflections at the triangular facets are modeled simulating facet contour and surface slope errors. The rays are then traced through the receiver aperture to the walls of the receiver. A PATRAN model of the receiver displays the energy per unit area on the receiver walls. The receiver is cylindrical (1.86 m diam by 2.99 m length) with a small aperture centered on one end to admit reflected solar rays. OFFSET was modified to calculate the flux density of the reflected energy within the receiver and to create the PATRAN file necessary to plot the receiver flux distribution maps. OFFSET also calculates the amount of power that misses the receiver aperture.

RESULTS

Three different thermal load cases were selected to predict the effects of thermal distortion on concentrator optical performance and to be compared with the effects of other error sources that influence optical performance. Facet deflections and rotations were predicted by the concentrator thermal and

structural models for each of the three thermal load cases and compared with the effects of facet flattening due to thermal loads and slope error. The selected points in time for the three cases represent 6 min, 30 min, and 54 min, respectively into the 57 min, sunlit portion of the fourth orbit, or approximately morning, noon, and dusk. Evaluation of the thermal results indicated that these times represent the worst temperature gradients for the beams and the approximate times for the maximum and minimum temperatures of the concentrator components during the sunlit portion of the orbit. In addition, the SD system has been predicted to reach full power by the fourth orbit and cyclic steady-state temperatures of the concentrator were reached by about the beginning of the third orbit thus providing the conditions present during normal operation.

The thermal analysis indicated that for thermal load cases 1, 2, and 3, the maximum temperatures of the box beams were 33, 60, and 75 °C (91, 140, and 167 °F), respectively. The maximum gradients through the box beams were 1.49, 1.05, 1.49 C/cm (6.8, 4.8, 6.8 F/in.) for cases 1, 2, and 3, respectively. The maximum temperatures of the facets were -2, 87, and 89 °C (29, 188, and 192 °F) for cases 1, 2, and 3, respectively. Note that the difference between the maximum and minimum facet temperatures per panel for all three cases was less than 10 °C (18 °F), while the difference between the maximum and minimum box beam temperatures was less than 8 °C (14 °F). The temperature difference between the facets and box beams per panel for all three cases was less than 40 °C (72 °F). Figure 11 shows the temperature distributions of the concentrator for the facets for thermal load case 2. Note that panels near the bottom of the concentrator, which have their normal almost parallel to the solar vector, are hotter than those on the top indicating that the panels' relative angle to the Sun has an influence on facet temperatures.

The structural analysis, which predicted the displacements and rotations of the facets, indicated that the maximum combined displacement of any facet node for the three cases was less than 0.15 cm (0.06 in.), which is small for a structure of this size. The results produced by CONRMS indicated that the concentrator rotational RMS values were 0.04, 0.12, and 0.17 mrad, for thermal load cases 1, 2, and 3, respectively. The maximum RMS value of 0.17 mrad is much smaller than the fabrication tolerances of 3 mrad.

The results of a separate finite element model of a facet under thermal loads indicate that the deflection of the facet center is less than 0.25 cm (0.1 in.), which results in a change of radius of curvature of 58.4, 76.1, 96.4, and 116.8 cm (23, 30, 38, and 46 in.) or a 3, 3.5, 3.9, and 4.3 percent increase for each of the four radii facet types. The facet model also indicated that the temperatures of standoffs are needed to accurately evaluate facet rotations.

To compare the effects of the thermally induced slope errors to other optical error sources, table 1 shows the power lost for the different cases of optical error. Power lost was defined to be the amount of power that misses the aperture and hits the aperture plate. Note that the design case with no slope error and no thermal distortion has about 0.47 kWt of power lost at the receiver. The thermal distortion effects of all three thermal load cases had little effect on this 0.47 kWt of power loss. The 3 mrad slope error causes the greatest amount of flux to hit the aperture plate. The amount of lost power actually decreased for the case where the facet flattened due to thermal loads because the outer radius of curvature of 2702 cm was actually under sized by about 508 cm (200 in.). As the facets flattened due to thermal

distortion, the increased radius of curvature became closer to the ideal radius of curvature, creating a smaller image at the aperture plane rather than the expected larger image. The combined case of thermal load case 2, facet flattening, and 3 mrad slope error again demonstrates that due to the thermal flattening of the facets, the amount of power lost decreases from the 3 mrad slope error case.

Figure 12 shows the flux distribution map on the receiver walls for the combined case. No significantly high flux rates were observed, with the maximum rate on the aperture plate being 5.7 W/cm^2 and the maximum rate on the receiver back wall being 3.8 W/cm^2. The flux distribution maps were for practical purposes identical for the three thermal load cases and the offset design case. Because the coefficient of thermal expansion is very small for the GFRP in the facets and box beams, close attention should be given to any material property changes as this may influence the amount of thermal distortion.

SUMMARY AND CONCLUSIONS

A method has been developed to provide an independent evaluation of the SD concentrator's thermal performance under different operating environments. This analytical method provides a way to predict the effects of thermal distortion on concentrator optical performance and includes performing thermal analyses to predict the temperature distributions of the concentrator, interfacing the thermal and structural models by mapping the thermal results onto the finite element model, performing structural analysis to predict the deformations of the concentrator under thermal loads, and producing flux distribution maps within the receiver cavity. The results indicate very minor thermal distortions occur during Space Station orbits, which have practically no influence on the performance of the concentrator, nor on the flux distributions within the receiver. A thermal analysis will be needed to predict if any hot spots develop within the receiver cavity. The very minor thermal distortion effects on concentrator optical performance indicates that from a thermal distortion standpoint the thermal design strategy and the selection of materials is good for the Space Station in low earth orbit.

REFERENCES

1. Irvine, T.B., Nall, M.M., and Seidel, R.C., 1986, "Solar Dynamic Power Systems for Space Station," Proceedings of the First NASA/DOD Control/ Structures Interaction Technology Conference, R.L. Wright, ed., NASA CP-2447-PT-1, pp. 149-166.

2. 1986, "Solar Concentrator Advanced Development Program, Task 1" NASA CR-179489.

3. Valade, F.H., 1988, "Space Station Solar Concentrator Development," Proceedings of the 1988 ASME Solar Energy Conference, ASME, New York, pp. 369-374..

4. Corrigan, R.D., and Ehresman, D.T., 1987, "Solar Concentrator Advanced Development Project," Energy - New Frontiers (22nd IECEC), Vol. 1, AIAA, New York, pp. 156-161.

5. 1983, "Thermal Radiation Analysis System, TRASYS II, Users Manual," MCR-73-105, Rev. 5, Martin Marietta.

6. Smith, J.P., 1983, "SINDA User's Manual," Rev. 3, COSMIC Program MSC-13805.

7. Winegar, S.R., 1987, "SINDA-NASTRAN Interfacing Program Theoretical Description and User's Manual," NASA TM-100158.

8. McCormack, C. W., ed., 1983, "MSC/NASTRAN User's Manual," Version 63, MacNeil-Schwendler Corp.

9. Jefferies, K.S., 1988, "Ray Tracing Optical Analysis of Offset Solar Collector for Space Station Solar Dynamic System," NASA TM-100853.

10. 1985, "PATRAN II User's Guide," Vol. I, II, and Enhancements., PDA Engineering, Santa Ana, CA.

TABLE 1. – POWER LOST DUE TO DIFFERENT OPTICAL ERRORS

Case description	Power lost, kW	Power lost, percent of total	Change in percent lost, percent
Offset design	0.4685	0.226	------
Facet flattening	.3081	.149	-0.077
Thermal load case 2 (noon)	.4730	.228	+.002
Facets w/3 mrad slope error	8.3713	4.042	+3.816
Combined - thermal load case 2, facet flattening, 3 mrad slope error	7.9308	3.830	+3.604

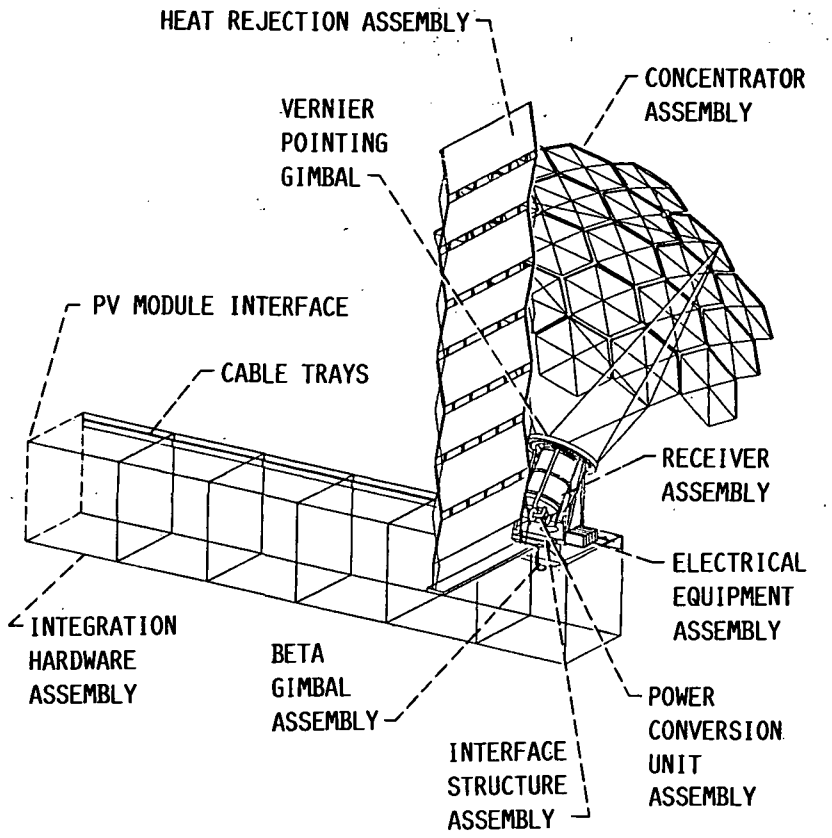

FIGURE 1. - SOLAR DYNAMIC MODULE.

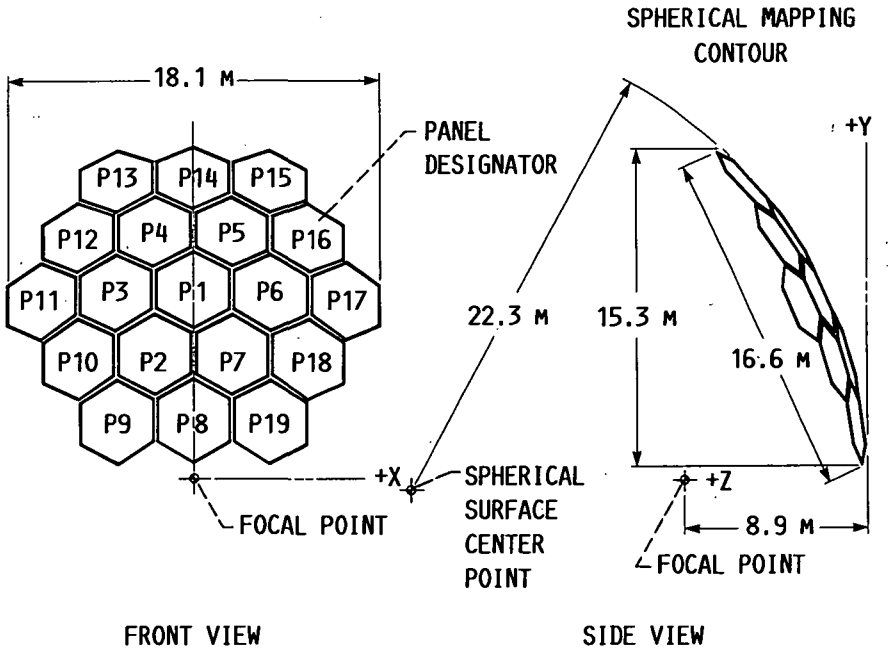

FIGURE 2. - AD CONCENTRATOR CONFIGURATION.

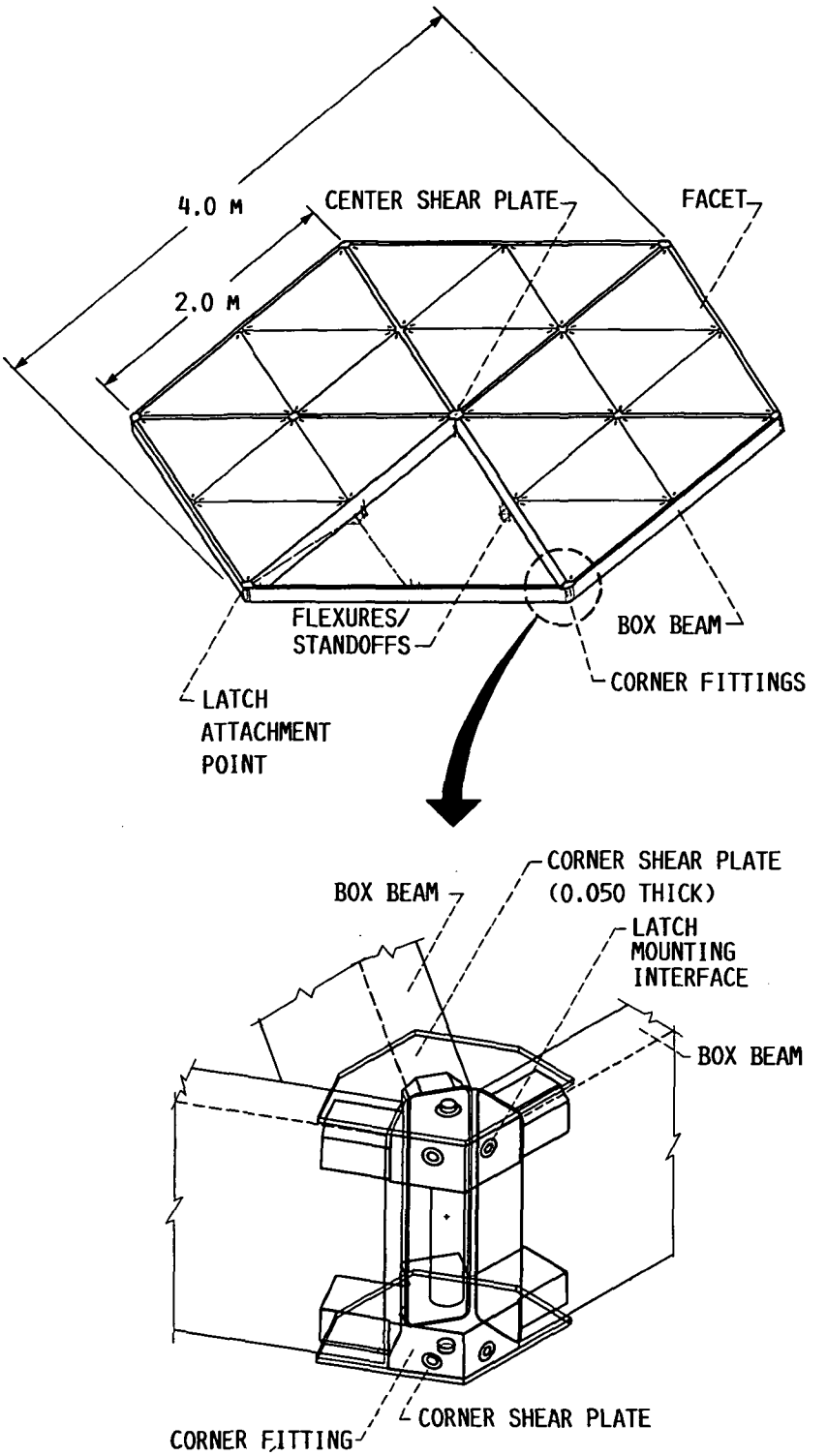

TYPICAL HEXAGONAL CORNERS WHERE THREE BOX BEAMS
ARE BONDED TO CORNER FITTINGS AND SHEAR PLATES

FIGURE 3. - HEXAGONAL PANEL DETAILS.

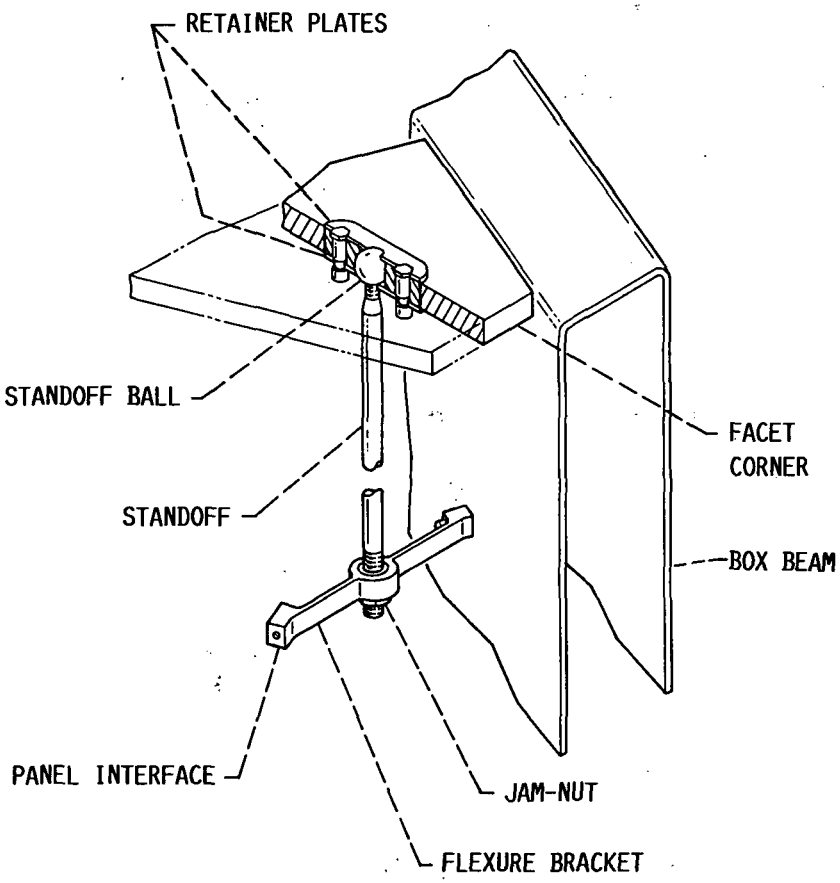

FIGURE 4. - DETAIL OF STANDOFF/FLEXURE ASSEMBLIES.

ORIGINAL PAGE IS
OF POOR QUALITY

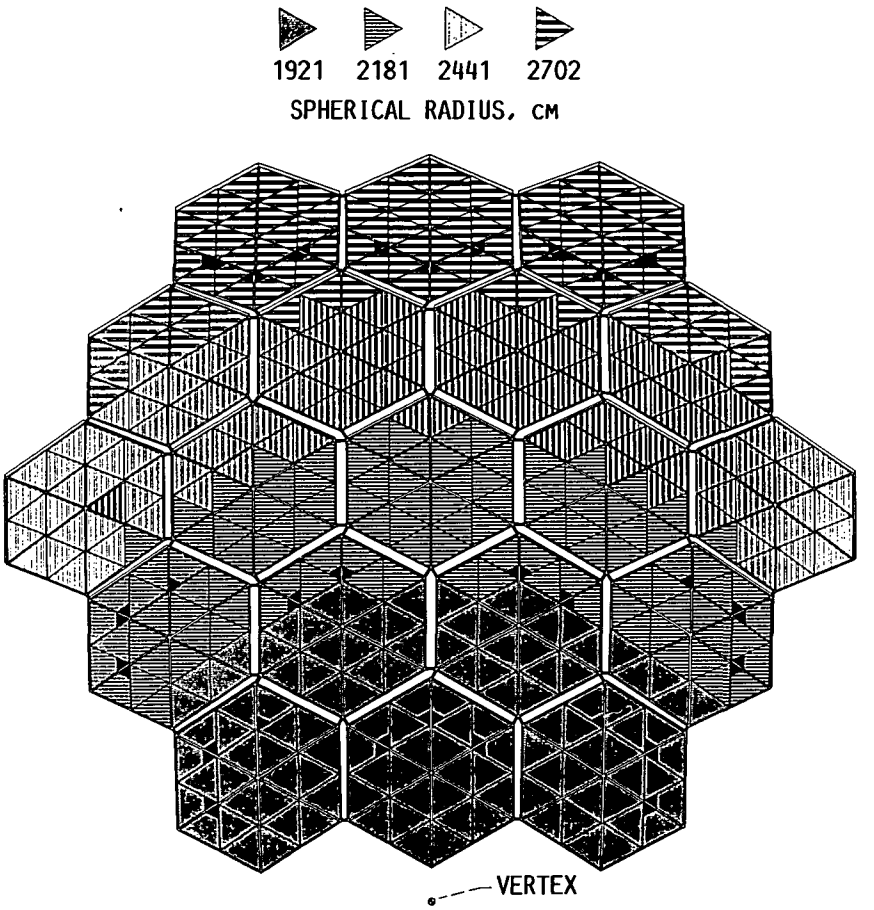

FIGURE 5. - AD CONCENTRATOR FACET RADII OF CURVATURE.

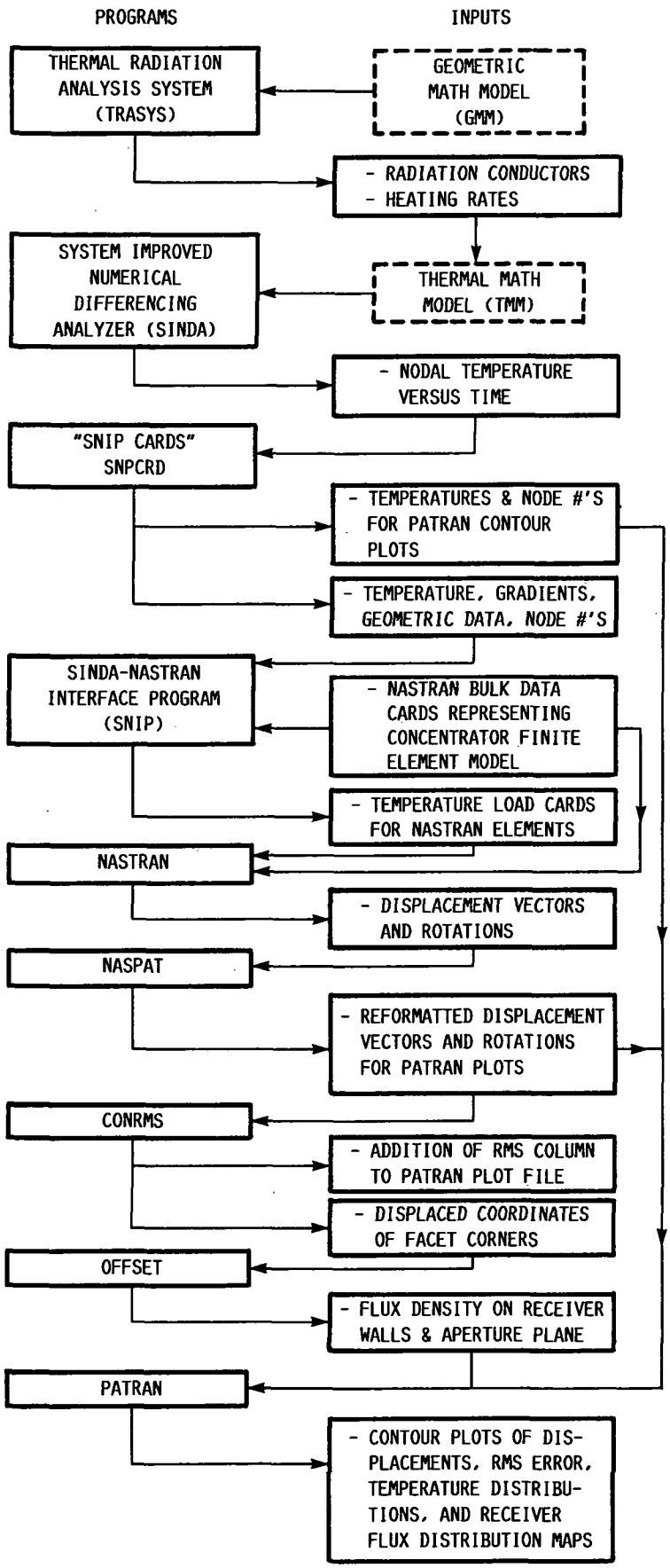

FIGURE 6. - PROGRAMS USED IN THERMAL DISTORTION ANALYSIS.

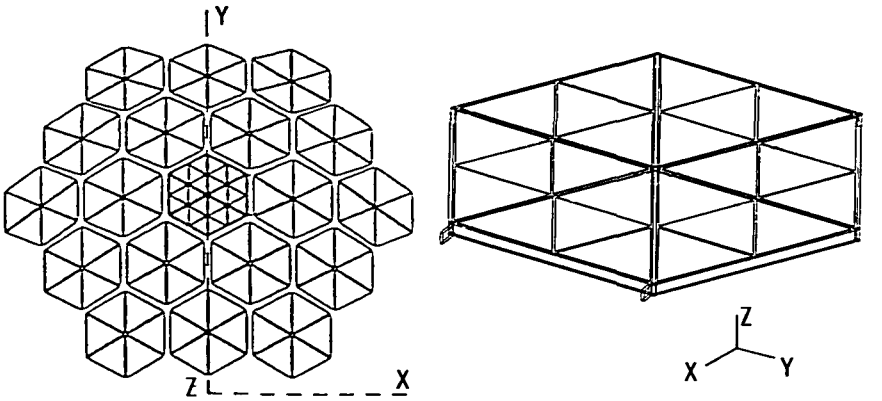

FIGURE 7. - CONCENTRATOR AND DETAILED PANEL GEOMETRIC MATH MODELS.

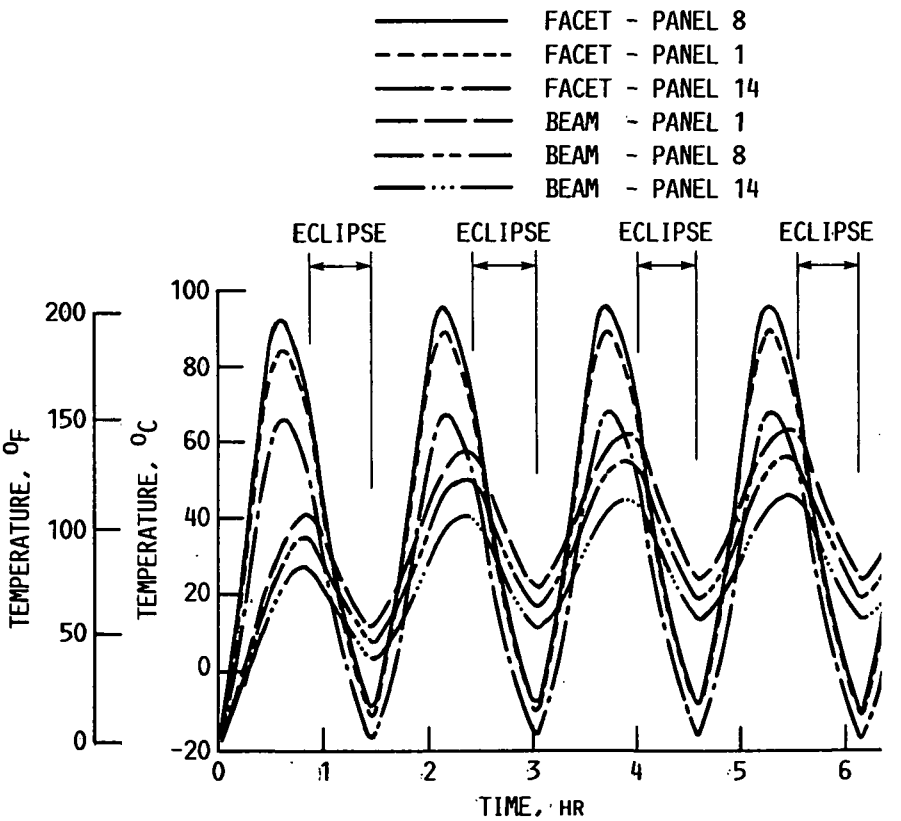

FIGURE 8. - AVERAGE FACET AND BEAM TEMPERATURE VERSUS TIME.

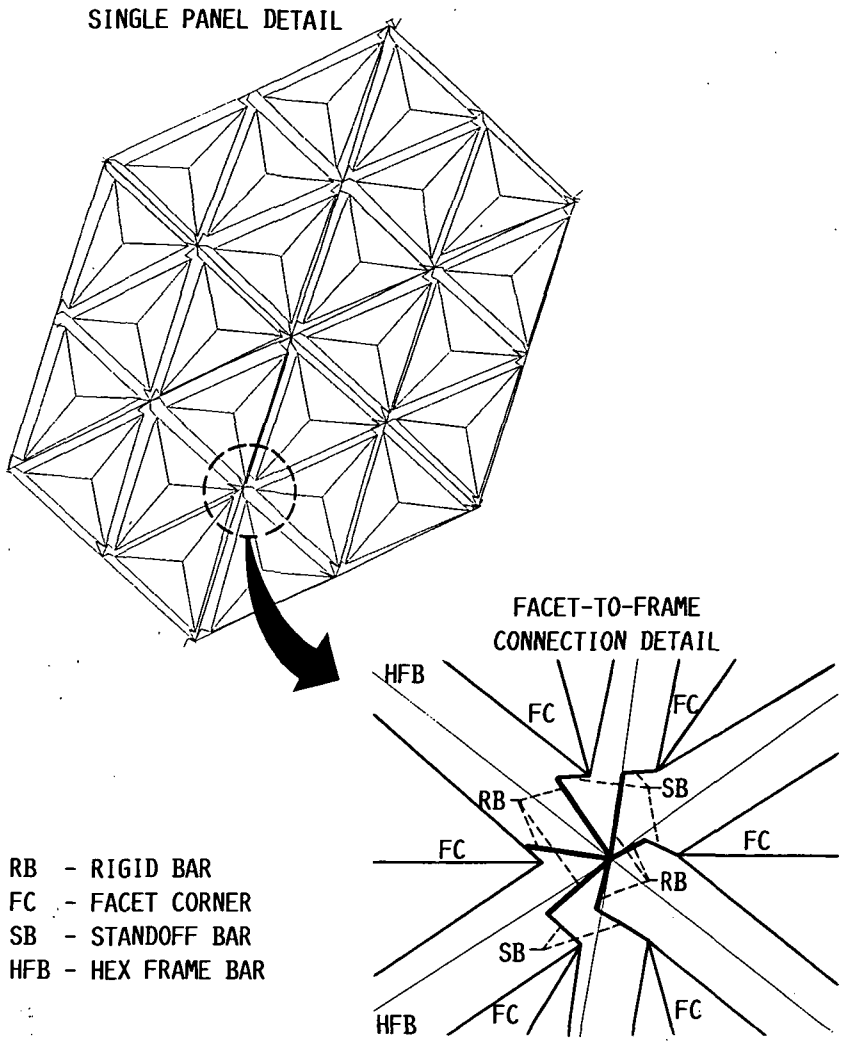

FIGURE 9. - DETAILS OF HEX PANEL FINITE ELEMENT MODEL.

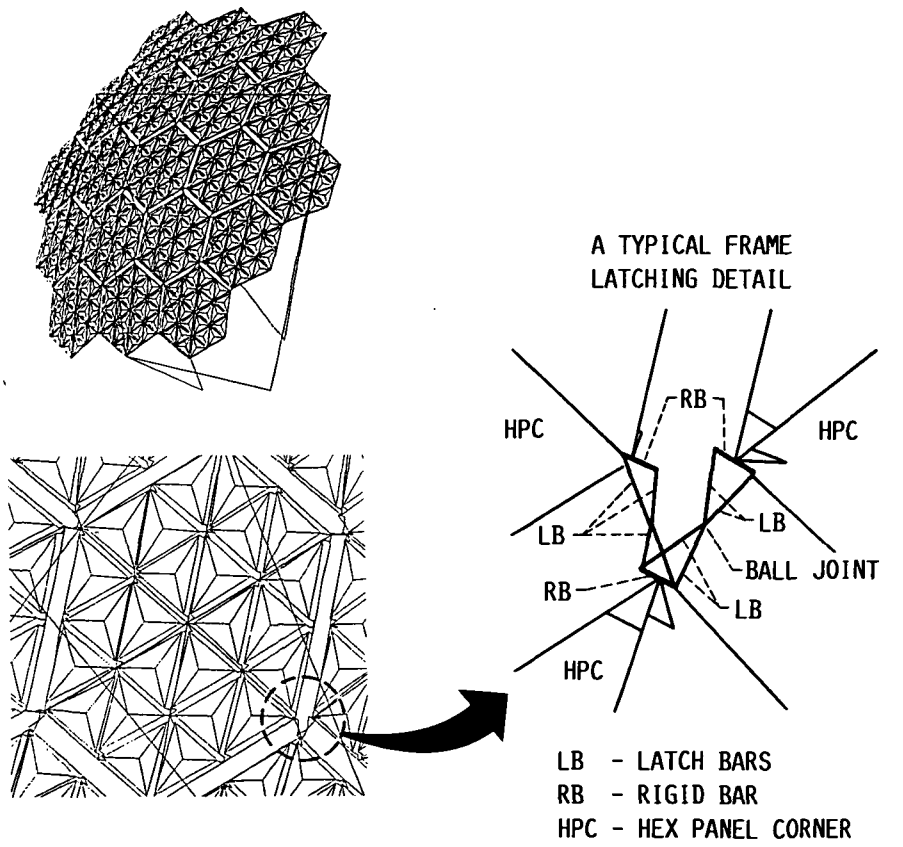

FIGURE 10. - FINITE ELEMENT LATCH MODEL DETAILS.

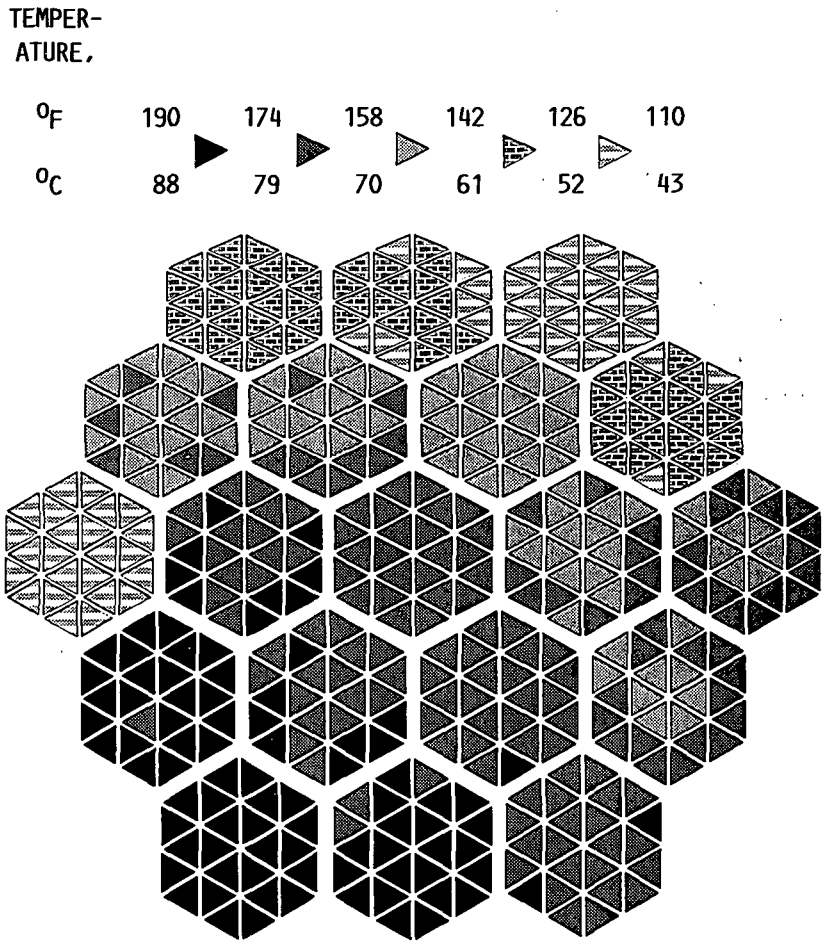

FIGURE 11. - CONCENTRATOR FACET TEMPERATURE DISTRIBUTION MAP FOR CASE 2.

ORIGINAL PAGE IS
OF POOR QUALITY

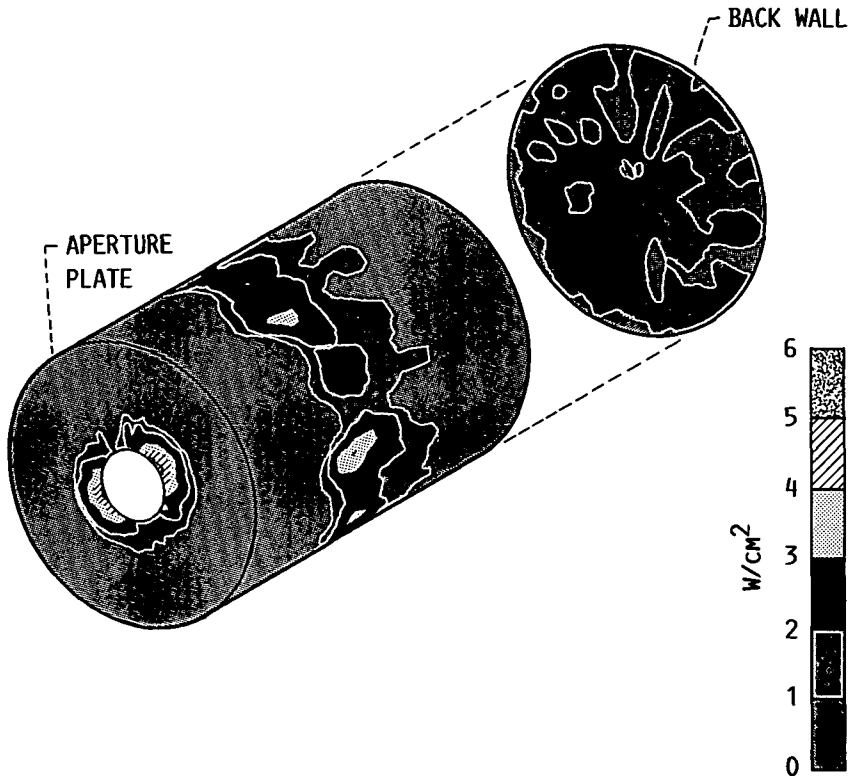

FIGURE 12. - FLUX DISTRIBUTION MAP WITHIN RECEIVER.

NASA
National Aeronautics and Space Administration

Report Documentation Page

1. Report No.	2. Government Accession No.	3. Recipient's Catalog No.
NASA TM-100868		

4. Title and Subtitle

Thermal Distortion Analysis of the Space Station Solar Dynamic Concentrator

5. Report Date

6. Performing Organization Code

7. Author(s)

Jeffrey J. Trudell, Vithal Dalsania, Joseph F. Baumeister, and Kent S. Jefferies

8. Performing Organization Report No.

E-4090

10. Work Unit No.

474-12-10

9. Performing Organization Name and Address

National Aeronautics and Space Administration
Lewis Research Center
Cleveland, Ohio 44135-3191

11. Contract or Grant No.

13. Type of Report and Period Covered

Technical Memorandum

12. Sponsoring Agency Name and Address

National Aeronautics and Space Administration
Washington, D.C. 20546-0001

14. Sponsoring Agency Code

15. Supplementary Notes

Prepared for the 23rd Intersociety Energy Conversion Engineering Conference cosponsored by the ASME, AIAA, ANS, SAE, IEEE, ASC, and AIChE, Denver, Colorado, July 31 - August 5, 1988. Jeffrey J. Trudell and Kent S. Jefferies, NASA Lewis Research Center; Vithal Dalsania, W.L. Tanksley & Associates, Lewis Research Center; Joseph F. Baumeister, Analex Corporation, Lewis Research Center.

16. Abstract

A method has been developed to evaluate the thermal distortion of the Space Station Solar Dynamic Concentrator and the effects of thermal distortion on concentrator optical performance. The analytical method includes generating temperature distributions with TRASYS and SINDA models, interfacing the SINDA results with the SINDA-NASTRAN Interface Program (SNIP), calculating thermal distortion with a NASTRAN/PATRAN finite element model, and providing flux distribution maps within the receiver with the ray-tracing OFFSET program. Temperature distributions, thermally induced slope errors, and flux distribution maps within the receiver are discussed. Results during a typical orbit indicate that temperatures of the hexagonal panels and triangular facets range between -18 °C and 99 °C (-1 to 210 °F), facet rotations are less than 0.2 mrad, and a change in facet radius due to thermal flattening is less than 5 percent. The predicted power loss with thermal distortion effects was less than 0.3 percent. The thermal distortion of the Solar Dynamic concentrator has negligible effect on the flux distribution within the receiver cavity.

17. Key Words (Suggested by Author(s))	18. Distribution Statement
Space station; Solar dynamics; Thermal distortion; Concentrators; Space power; Temperature; TRASYS; SINDA; NASTRAN	Unclassified - Unlimited Subject Category 20

19. Security Classif. (of this report)	20. Security Classif. (of this page)	21. No of pages	22. Price*
Unclassified	Unclassified	22	A02

NASA FORM 1626 OCT 86

*For sale by the National Technical Information Service, Springfield, Virginia 22161

National Aeronautics and
Space Administration

Lewis Research Center
Cleveland, Ohio 44135

Official Business
Penalty for Private Use $300

FOURTH CLASS MAIL

ADDRESS CORRECTION REQUESTED

U.S.MAIL

Postage and Fees Paid
National Aeronautics and
Space Administration
NASA 451

NASA